Active Traffic Management on Road Networks: A Macroscopic Approach

By Alex A. Kurzhanskiy and Pravin Varaiya

University of California, Berkeley, CA

Active Traffic Management (ATM) is the ability to dynamically manage recurrent and nonrecurrent congestion based on prevailing traffic conditions in order to maximize the effectiveness and efficiency of road networks. It is a continuous process of (1) obtaining and analyzing traffic measurement data; (2) operations planning—simulating various scenarios and control strategies; (3) implementing the most promising control strategies in the field; and (4) maintaining a real time decision support system that filters current traffic measurements to predict the traffic state in the near future, and to suggest the best available control strategy for the predicted situation. ATM relies on a fast and trusted traffic simulator for the rapid quantitative assessment of a large number of control strategies for the road network under various scenarios, in a matter of minutes. The open source macrosimulation tool Aurora Road Network Modeler is a good candidate for this purpose. The paper describes the underlying dynamical traffic model and what it takes to prepare the model for simulation; covers the traffic performance measures and evaluation of scenarios as part of operations planning; introduces the framework within which the control strategies are modeled and evaluated; and presents the algorithm for real time traffic state estimation and short term prediction.

Keywords: Active Traffic Management, Macroscopic Traffic Model, Hierarchical Control, Set-Valued Estimation

1. Introduction

Traffic congestion is a source of productivity and efficiency loss, wasteful energy consumption and excessive air pollution. Continued travel demand growth and budget constraints have made it difficult for transportation agencies to increase roadway capacity in major metropolitan areas. Active Traffic Management (ATM) is the ability to dynamically manage recurrent and nonrecurrent congestion based on prevailing traffic conditions without capacity growth. It makes use of automated systems and human intervention to manage the traffic in order to maximize the effectiveness and efficiency of road networks. This paper proposes a certain structure of ATM and focuses on some of its components. It stems from the authors' engagement in the TOPL research project conducted at Berkeley since 2006 [18]. TOPL seeks to assist the California Department of Transportation improve the operation of California freeways.

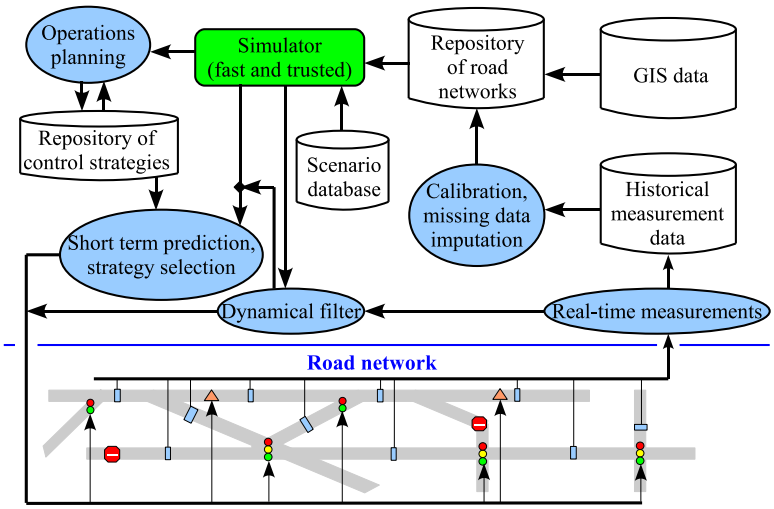

Figure 1. ATM workflow diagram.

ATM is the cycle consisting of (1) continuous traffic measurement and measurement data analysis, without which any attempt to manage a road network would be blind; (2) operations planning, which includes evaluating the road network performance under various scenarios, such as demand increase, lane closures, special events, etc., developing control strategies that improve performance, and testing these strategies in terms of their cost and the benefits they bring; (3) implementing the most effective of these control strategies by installing necessary hardware and software in the field; and (4) running the decision support system in real time, which includes filtering the measurement data, providing short term prediction of the traffic state, and selecting the best available control strategy for the next one or two hours.

The ATM workflow diagram is presented in Figure 1. It relies on a communication network that feeds real time measurements from the field elements in the road network to the traffic control center and transfers commands generated by the control software (and human operators) to the actuators in the field. The central element of the ATM workflow is the 'fast and trusted simulator'. The simulator is trusted because it is founded on sound theory of traffic flow; it is parsimonious, only including parameters that can be estimated; and it is tested for reliability. As a candidate for such simulator, we propose Aurora Road Network Modeler (RNM) [1], an open-source tool set for modeling road networks that can include freeways and arterials with signalized intersections. The underlying *macroscopic* dynamical traffic model and the way it is built using GIS (Geographic Information Systems) and historical measurement data is explained in Section 2.

The simulator has three modes of operation. In the first or *operations planning* mode, a large number of simulations are run to evaluate scenarios and test potential operational improvements on the already prepared and calibrated road network. Scenarios incorporate known events such as a football game or a confirmed accident, or future events considered plausible on the basis of statistical inference and learning techniques that combine historical data with the current estimate of the state of the system (e.g., likelihood of an accident occurring in a certain location, conditional on the current congestion state, rain or fog conditions). The configurations for the implemented control strategies are stored in the repository, readily accessed by the real time decision support system. Section 3 touches the subject of operations planning, while Section 4 focuses on the control structure and modeling. The second mode of operation is the *dynamical filter*: the simulation, with

some uncertainty in system parameters and inputs, runs in real time as the noisy measurements arrive from the traffic sensors. By filtering the measurement data through the simulation, the traffic state is estimated and fed back into the traffic responsive control algorithms. The third mode of operation is the *short term prediction and strategy selection*: with the initial conditions coming from the filtered measurements and predicted with some uncertainty in short term future inputs, the simulator runs a number of plausible near term scenarios with available control strategies and calculates the resulting congestion and potentially serios stresses. The strategy promising the greatest benefits, is deployed by sending the corresponding commands to the actuators in the field. Section 5 describes the traffic state estimation and prediction.

2. Dynamical Model of Traffic

(*a*) *Model Description*

We start by introducing the traffic model employed by our trusted simulator [1], which is based on the Cell Transmission Model [3; 4].

The road network consists of directed links and nodes, where links represent stretches of roads and nodes connect the links. Denote by $\mathcal{L}$ the set of links, and by $\mathcal{N}$ the set of nodes in the network. A node must always have at least one input and at least one output link. A link is called an *ordinary link*, if it has both begin and end nodes. A link with no begin node is a *source link* or *source*, and a link with no end node is a *destination link* or *sink*. Each link $l \in \mathcal{L}$ is characterized by its length Δx_l, number of lanes k_l, and the fundamental diagram (capacity F_l, free flow speed v_l and congestion wave speed w_l, see Figure 2)†, which takes into account the number of lanes. Sources are the links through which the vehicles enter the system, and therefore have demand profiles assigned to them. Each node $\nu \in \mathcal{N}$ is characterized by a split ratio matrix $\mathcal{B}_\nu$ that determines how the incoming flows are distributed among the output links. Nodes may be used not only to represent intersections, merge, or diverge points, but also to break up long links into smaller ones.

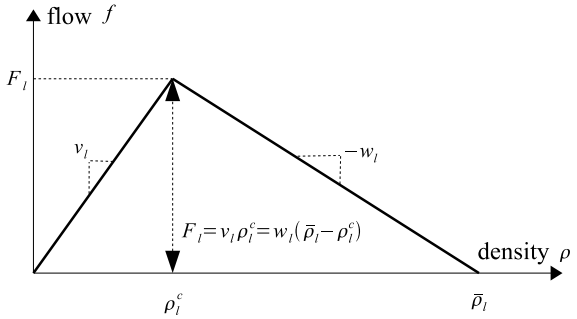

Figure 2. Fundamental diagram associated with some link l.

† The fundamental diagram is a density-flow function, usually concave. In our case, it has the triangular shape of Figure 2, defined by three values: capacity (maximum number of vehicles per hour the link can let through) F_l, the free flow speed (the average vehicle speed in the link measured under low traffic density conditions) v_l, and the congestion wave speed (the speed with which congestion wave propagates backward) w_l. Alternatively, one could specify the triangular fundamental diagram as a triplet: capacity F_l, critical density (number of vehicles per mile in the link at which the capacity is reached) ${\rho^c}_l$, and jam density (number of vehicles per mile in the link at which traffic can no longer move) $\bar{\rho}_l$.

In the simple example of a single-directional freeway of Figure 3, nodes are places where on-ramps merge into and off-ramps diverge from the freeway, or where freeway characteristics, such as the number of lanes, change; ordinary links are the stretches of freeway going from node to node; sources are on-ramps; and sinks are off-ramps.

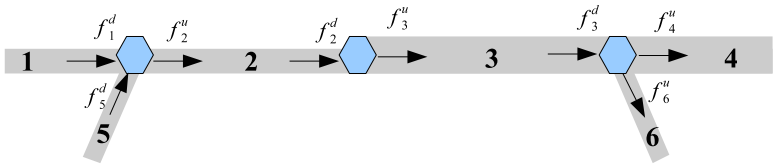

Figure 3. Simple road network: links are numbered from 1 to 6, nodes are shown in light blue.

The state of the road network at time t is described by the vehicle density in each link, $\rho_l(t)$. Given some initial condition, which usually comes from measurements, $\rho_l(t_0) = \rho_l^0$, the system evolves in time according to

$$\rho_l(t + \Delta t) = \rho_l(t) + \frac{\Delta t}{\Delta x_l} \left({f^u}_l(t) - {f^d}_l(t) \right), \tag{2.1}$$

where Δt is the size of the time step, satisfying the condition $\Delta t \leq \min_l \left\{ \frac{\Delta x_l}{v_l} \right\}$; ${f^u}_l(t)$ and ${f^d}_l(t)$ are upstream (entering link l) and downstream (exiting link l) flows respectively. For sources, ${f^u}_l(t) = r_l(t)$, where $r_l(t)$ is the value of demand—the flow that desires to enter the system through source link l at time t. For sinks, ${f^d}_l(t) = v_l \rho_l(t) \min \left\{ 1, \frac{F_l}{v_l \rho_l(t)} \right\}$. For ordinary links, ${f^u}_l(t)$ is determined by the begin node and ${f^d}_l(t)$ is determined by the end node of link l.

A node with m input and n output links has $m \times n$ split ratio matrix $\mathcal{B}_\nu(t) = \{\beta_{ij}(t)\}_{i=1..m}^{j=1..n}$. This matrix is nonnegative, its elements lie in the interval $[0, 1]$, and the sum of the elements in each row equals 1. The element $\beta_{ij}(t)$ defines the portion of the vehicle flow coming from input link i that has to be directed to the output link j at time t. Input flows ${f^d}_i(t)$ and output flows ${f^u}_j(t)$, $i = 1..m$, $j = 1..n$, for the node are computed in steps 1-7 that follow.

1. Compute supply for each output:
$$s_j(t) = \min \left\{ F_j, w_j \left(\overline{\rho}_j - \rho_j(t) \right) \right\}, \quad j = 1..n, \tag{2.2}$$
where F_j is the capacity, w_j is the congestion wave speed, $\overline{\rho}_j$ is the jam density, and $\rho_j(t)$ is the current density of the output link j.

2. Set index $q = 0$.

3. Compute input demands:
$$\tilde{d}_i^{[q]}(t) = v_i \rho_i(t) \min \left\{ 1, \frac{F_i}{v_i \rho_i(t)} \right\}, \quad i = 1..m, \tag{2.3}$$
where F_i is capacity, v_i is free flow speed, and $\rho_i(t)$ is the current density of the input link i. Quantity $\tilde{d}_i^{[0]}(t)$ represents the desired flow from the input link i.

4. Compute output demands:
$$d_j^{[q]}(t) = \sum_{i=1}^{m} \beta_{ij}(t) \tilde{d}_i^{[q]}(t), \quad j = 1..n. \tag{2.4}$$
Quantity $d_j^{[0]}(t)$ represents the total flow that desires to enter the output link j.

5. For $q = 1..n$, repeat

   (a) scale down input demands to satisfy the output supply if necessary:

$$\tilde{d}_i^{[q]}(t) = \begin{cases} \tilde{d}_i^{[q-1]}(t), \text{ if } \beta_{iq}(t) = 0 \\ \tilde{d}_i^{[q-1]}(t) \min\left\{1, \frac{s_j(t)}{d_j^{[q-1]}(t)}\right\}, \text{ otherwise} \end{cases}, \quad i = 1..m; \quad (2.5)$$

   (b) recompute output demands $d_j^{[q]}(t)$, $j = 1..n$, according to (2.4).

   This step implements the proportional priority rule for merging links and the first-in-first-out rule for diverging links as they are stated in [4]†.

6. Flow leaving the input link i is

$$f^d{}_i(t) = \tilde{d}_i^{[n]}(t) \quad i = 1..m. \quad (2.6)$$

7. Flow entering the output link j is

$$f^u{}_j(t) = \sum_{i=1}^{m} \beta_{ij} \tilde{d}_i^{[n]}(t), \quad j = 1..n. \quad (2.7)$$

(*b*) *Building the Model*

Building a model that is ready for simulation consists in (1) putting together a road network by creating nodes and links with correct lengths and lane counts; (2) calibrating the system, that is, assigning a fundamental diagrams to each link; (3) defining time-varying demand functions for the source links and split ratio matrices for the nodes. This is generally a time-consuming process, as no single data source provides the information necessary for all three tasks.

The starting point of the process is obtaining the GIS data about the roads of interest from available commercial [9; 17] or free [10] sources. GIS data comes in the form of shape files with information about the street segments that can be converted into link-node description. Aurora RNM [1] has a utility called GIS Importer that performs this task. In special cases, for example, freeways of California or freeways of Portland region in Oregon, we are lucky to have single sources, PeMS [14] and PORTAL [15] for the freeway geometry and for the traffic measurement data.

Measurement data from the freeway detectors provided by information systems such as PeMS [14] or PORTAL [15] allows to estimate fundamental diagrams for the corresponding freeway links. The full description of the calibration algorithm is given in [5]. Here we provide a summary.

1. For each *reliable*‡ detector on the selected stretch of freeway, extract available historical density and flow measurements. The distance between detectors is often larger than the link size in our model. Hence, the retreived detector data may apply (and usually does) to more than one link.

2. Find maximum measured flow value. Usually, this will be the capacity value F_l.

3. Use least squares method to estimate free flow speed v_l. Practice shows that free flow density-flow pairs give a good fit. Set critical density $\rho^c{}_l = \frac{F_l}{v_l}$.

4. Use constrained least squares method to determine congestion wave speed w_l.

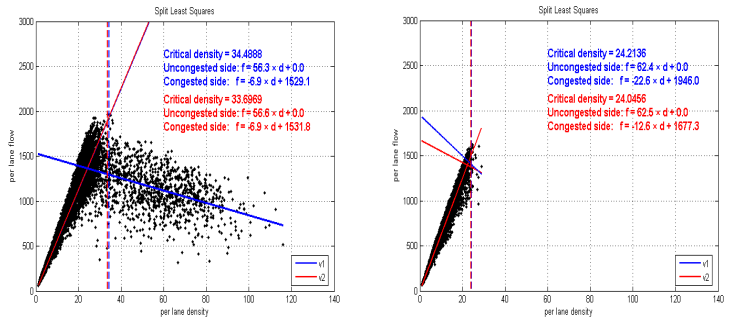

(a) (b)

Figure 4. Estimating fundamental diagram: (a) good data; (b) poor data.

When detector data are good, steps 1-4 produce a decent result (Figure 4a). If, on the other hand, detector data are poor due to malfunctioning detector or just because the capacity is never reached at this point of freeway (Figure 4b), then we can either use fundamental diagrams from the neighboring links or impute the missing data as suggested in [2] and repeat steps 2-4.

The most difficult part of calibrating urban streets or arterials is to estimate their capacities. Once the capacity of an arterial link is determined from available measurements or intelligent guess, the free flow speed can be set to the speed limit assigned on that street, and the jam density can be derived from estimating the number of vehicles this link can store and dividing this number by the length of the link.

Finally, it remains to define the demand functions for the sources and split ratio matrices for the nodes. For freeways, systems like PeMS [14] and PORTAL [15] should provide on-ramp flow data that could be used to construct the demand functions. The split ratios should be computed from the measurements of the mainline and off-ramp flows: in the example shown in Figure 3 these would be the measurements of flows $f^u{}_4$ and $f^u{}_6$. In practice, however, on- and off-ramp flows may not be available, which is currently the case for some California freeways. The demands and split ratios must then be imputed so that when used in the model, the model produces mainline flows that match the measurements. As most inverse problems, the problem of the demand and split ratio imputation is ill-posed in the sense of Hadamard: its solution is not unique. One has to impose certain restrictions on the demand and split ratio values and demand variations. The imputation problem is thoroughly covered in [8].

Obtaining demand and split ratio data for arterials is a challenge. Sources of this information vary from city to city. In California we have to rely on regional planning agencies such as MTC in San Francisco Bay Area, or SANDAG in San Diego.

3. Operations Planning

The objective of the operations planning is to develop strategies that improve traffic performance on congested road networks. The foundation of operations planning is the monitoring of traffic in the areas of interest and analysis of the measurement data. Such analysis pinpoints the weaknesses in travel corridor operations, indicates

† Proportional priority rule means that each output link accomodates vehicles from the input links proportionally to the input demands. First-in-first-out rule means that the input-to-output flows in the node should always be in proportion to each other defined by the split ratio matrix.

‡ PeMS [14], for example, provides day by day health status for each detector.

bottlenecks and accident hot spots, and provides hints about possible strategies of congestion relief.

The devised strategies may involve expanding capacity at the bottleneck by adding extra lane(s), or such operational techniques as *demand management*, which focuses on reducing the excess demand during peak hours; *incident management*, which targets resources to alleviate incident hot spots; providing *traveler information*, which seeks to reduce traveler buffer time—the extra time the travelers must add to their average travel time when planning trips to ensure on-time arrival; *traffic flow control*, which implements ramp metering at freeway on-ramps near locations where significant reductions of congestion are likely to occur; imposing *variable speed limit* (VSL) on freeways to homogenize the flow during peak hours; and optimizing *signal timing plans* at signalized intersections. Operations planning needs quick quantitative assessment of the performance benefits that can be gained from the congestion relief strategies, in order to rank them and, combined with a separate estimate of the deployment cost of these strategies, select the most promising of them based on benefit/cost ratios or the magnitude of benefits.

General link performance measures are listed below.

- *Traffic speed*, measured in miles per hour (mph):
$$V_l(t) = \frac{{f^d}_l(t)}{\rho_l(t)}. \tag{3.1}$$
- *Instantaneous Travel Time*, measured in hours—the travel time through the link that would occur if traffic speed in the link stayed constant at its value at current time t, $V(t)$:
$$ITT_l(t) = \frac{\Delta x_l}{V_l(t)}. \tag{3.2}$$
- *Actual Travel Time*, measured in hours—the travel time computed using actual speed values past current time t:
$$ATT_l(t) = T_l(t)\Delta t, \tag{3.3}$$
where
$$T_l(t) = \arg\max_{\tau} \left\{ \sum_{\tau'=0}^{\tau-1} V_l(t+\tau')\Delta t \le \Delta x_l \right\}. \tag{3.4}$$
- *Vehicle Miles Traveled (VMT)* is the measure of the throughput of the link during current time step:
$$VMT_l(t) = \rho_l(t)V_l(t)\Delta x_l \Delta t. \tag{3.5}$$
- *Vehicle Hours Traveled (VHT)* reflects the number of vehicles in the link during current time step:
$$VHT_l(t) = \rho_l(t)\Delta x_l \Delta t. \tag{3.6}$$
- *Delay* measured in vehicle-hours (vh):
$$D_l(t) = VHT_l(t) - \frac{VMT_l(t)}{v_l(t)}. \tag{3.7}$$
- *Productivity Loss*, measured in lane-mile-hours (lmh)—the degree of underutilization of the link lanes due to congestion:
$$PL_l(t) = \begin{cases} 0, & \text{if } V_l(t) = v_l, \\ \left(1 - \frac{{f^d}_l(t)}{F_l}\right) k_l \Delta x_l \Delta t, & \text{otherwise.} \end{cases} \tag{3.8}$$

All these performance values, except for the actual travel time, can be computed at run time of the dynamical system. Computation of the actual travel time requires the knowledge of the whole dynamical system trajectory. Knowing actual travel time, VMT, VHT, delay and productivity loss for each individual link, one can compute the same quantities for any specifyed route in the network.

Arterial links whose end nodes are signalized intersections have additional performance measures: *delay per cycle*—number of vehicle-hours spent waiting at the signal; *queue size*—number of vehicles in the link; *phase utilization*—percent of the green phase time used during cycle; *cycle failure*—percent of vehicles waiting for more than one red light; *flow to capacity ratio*, which characterizes the utilization of the available capacity; and *progression quality*—percent of vehicles arriving during the green phase. Knowing these performance measures for each incoming link of an intersection, one can assess the overall performance of the intersection.

To evaluate the road network performance under different scenarios, such as incidents, lane closures, special events, demand fluctuations, etc., using the macroscopic traffic model (2.1)-(2.7), we use 'switches' in the model parameters (fundamental diagrams at links and split ratio matrices at nodes) or inputs (demands at source links) at specified times.

Switches in fundamental diagrams model incidents and lane closures. For example, suppose the original fundamental diagram of some link l is $F_l = 6000$ vehicles per hour (vph), $v_l = 60$ mph, $w_l = 15$ mph, and an accident blocking half of the lanes occurs at 10 o'clock and lasts until 10.30 when the road is cleared. To model this accident one has to specify two switches in the fundamental diagram: $F_l(10) = 3000$ representing the capacity drop, and $F_l(10.5) = 6000$ representing the return to normal operation. Evaluating the impact of faster reaction times (how much better would the system perform if the accident were cleared in 20 minutes instead of 30?) is part of incident management. One can also use switches in the fundamental diagrams to study the benefit of opening shoulders as general purpose lanes near bottlenecks during peak hours.

Special events and the impact of providing traveler information are modeled by switches in the split ratio matrices at given nodes. A change in the proportion of traffic flow directed into certain output link of a node may create a bottleneck and cause a congestion upstream of this node. Demand fluctuations are modeled by applying some nonnegative coefficients to the original demand functions assigned to given sources.

In Aurora RNM these switches in parameters and inputs are implemented as events that can be generated by the user and triggered at user-specified times during the simulation. The impact of each scenario can be quickly assessed, as Aurora RNM Simulator computes the general performance measures for links and routes.

Another important aspect of the operations planning, as well as real time decision support, is the evaluation of the traffic flow control technologies, considered next.

4. Control of Traffic Flow

Among the components of the congestion relief strategies mentioned in the previous Section, demand management, incident management and traveler information influence the traffic indirectly: they affect the inputs and the parameters of the system in a way that can be estimated but not measured exactly. Direct and measurable influence over traffic behavior is achieved through traffic flow control.

In the macroscopic link-node model (2.1)-(2.7), the link state evolves in time according to the law of conservation, for any link l with an end node, whereas the flow $f^d{}_l$ exiting this link can be potentially restricted by the node. (By definition, the flow exiting a destination link is restricted only by the capacity of that destination link.) So nodes are the network components where traffic flow control can be imposed.

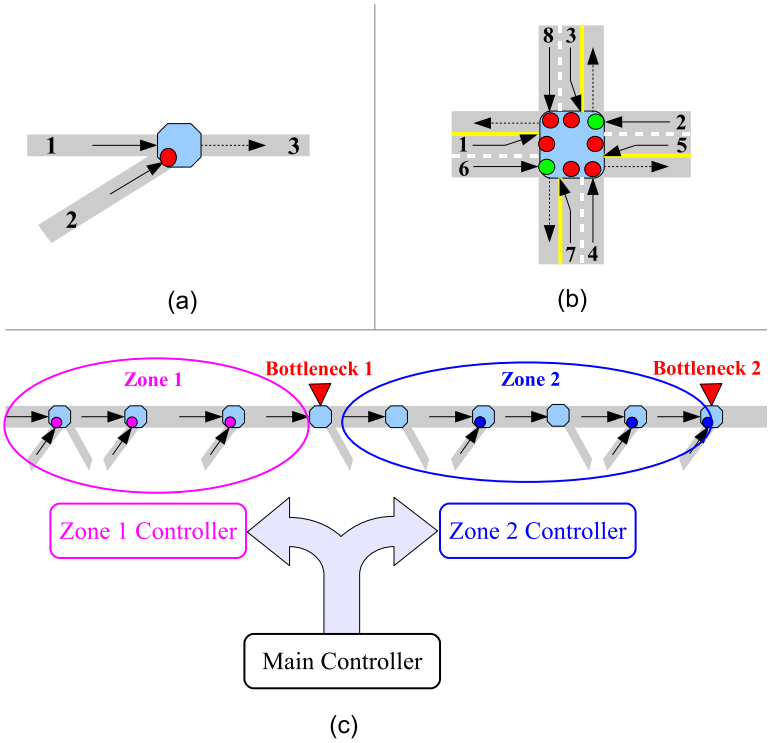

Figure 5. Controller hierarchy: examples of (a) local controller (ramp meter); (b) node controller (signalized intersection); (c) complex controller (coordinated ramp metering).

We propose the controller hierarchy that is summarized in Figure 5.

- *Local* controller is assigned to a particular input link of a node and controls only the flow coming from that link. An example of a local controller is a ramp meter shown in Figure 5a. Here, the node has two input links, uncontrolled freeway link 1 and controlled on-ramp 2.

- *Node* controller is assigned to a node and controls the flows coming from all the input links of that node. An example of a node controller is a signalized intersection shown in Figure 5b. Here, only two non-conflicting input flows (1 and 5, 2 and 6, 3 and 7, or 4 and 8) are allowed at any one time, while the others are blocked. The individual input flows are still controlled each by its own local controller, but now the local controllers are synchronized by the centralized node control.

- *Complex* controller operates on multiple local, node, or even other complex controllers coordinating their action toward some common objective. An example of a complex controller is a coordinated ramp metering system shown in Figure 5c. This is a freeway with two identified bottlenecks, which divide the freeway into zone 1 and zone 2, each ending at the corresponding bottleneck.

Bottlenecks are expected to move throughout the day. Zone controllers are responsible for coordinating local ramp meters at the on-ramps within their respective zones, whereas the main controller keeps track of the bottleneck locations and zone configuration. Main and zone controllers are both complex controllers.

The model (2.1)-(2.7) incorporates a controller action by replacing the formula (2.3) for input demands with

$$\tilde{d}_i^{[0]}(t) = v_i \rho_i(t) \min\left\{1, \frac{F_i}{v_i \rho_i(t)}, \frac{C_i(t, \boldsymbol{\rho}(t))}{v_i \rho_i(t)}\right\}, \quad i = 1..m, \tag{4.1}$$

where m is the number of input links in a node, $\boldsymbol{\rho}(t)$ in bold represents the entire system state of densities in all the links in the network, and $C_i(t, \boldsymbol{\rho}(t))$ is the control function for the flow entering the node from input link i.

The control may be open-loop, $C_i(t, \boldsymbol{\rho}(t)) = C_i(t)$, or closed-loop. The simplest example of an open-loop controller is the time-of-day (TOD) local ramp meter, that restricts the flow coming from an on-ramp link by some constant value that changes several times during the day. A pre-timed signal with fixed offset, time cycle and phases, operating on an arterial intersection is an example of an open-loop node controller.

Closed-loop control responds to the traffic state and can potentially adapt to the special situations such as incidents. An example of a closed-loop controller is ALINEA [11], a local ramp meter which for the configuration in Figure 5a is defined by the formula

$$A_2\left(t, \rho_3(t)\right) = A_2\left(t - \Delta t, \rho_3(t - \Delta t)\right) + v_3\left({\rho^c}_3 - \rho_3(t)\right), \tag{4.2}$$

where subscripts '2' and '3' refer to links 2 and 3 respectively, and A_2 is the ALINEA flow rate. It is generally a good idea for a controller such as ALINEA to work in conjunction with a queue controller that prevents the vehicle queue on the ramp from growing too much, causing traffic spillback further upstream. The most common queue controller uses the queue override algorithm:

$$Q_2\left(t, \rho_2(t)\right) = {f^u}_2(t) + \frac{v_2}{\Delta x_2}\left(\rho_2(t) - {\rho^c}_2\right), \tag{4.3}$$

where Q_2 is the flow rate prescribed by queue override controller. Having both ALINEA and queue override active at the same time, the local ramp meter computes its rate as

$$C_2(t, \boldsymbol{\rho}(t)) = \max\left\{A_2\left(t, \rho_3(t)\right), Q_2\left(t, \rho_2(t)\right)\right\}. \tag{4.4}$$

Coordinated ALINEA, known as HERO [13], whose idea is to first apply ALINEA algorithm (4.2) to the on-ramp closest to the bottleneck until the queue limit is reached, then turn on ALINEA at the next on-ramp upstream until the queue limit is reached there, and so on, is a closed-loop complex controller. An example of a closed-loop complex controller that coordinates multiple node controllers operating on signalized arterial intersections is TUC [6].

Variable speed limit or VSL control also influences the traffic flow from the nodes. If some arbitrary VSL controller calculates the desired speed limit v_l^* for link l, the flow rate prescribed by the corresponding local controller is

$$C_l(t, \rho_l(t)) = v_l^* \rho_l(t). \tag{4.5}$$

It is often the case that while being tested in simulations, closed-loop controllers greatly improve the system performance reducing delay and productivity loss, but after deployment of these controllers in the field, the results are disappointing.

The reason is the poor quality of the feedback signal from noisy or malfunctioning sensors, or the lack of feedback altogether in the real world. For example, PeMS [14] detector health reports indicate that up to 30% of California freeway loop detectors are not fully functional throughout the year.

To simulate feedback control algorithms and test their performance in a setting that resembles the real world situation, we propose to incorporate sensors into the traffic model. We call this concept *virtual sensors*. Virtual sensors model the work of measurement devices reporting vehicle counts and/or speeds from particular road network locations based on simulated link data. Within each such virtual sensor one can adjust the noise level and choose the sensing quality in the range from excellent to unsatisfactory. The data reported by these virtual sensors are used by the closed-loop traffic flow control. Figure 6 summarizes the idea on the high level. In the ideal setting (Figure 6a) the controller has access to the current system state directly from the state equation (2.1). Introducing virtual sensors, we replace the *state feedback* with the *measurement feedback* in the model.

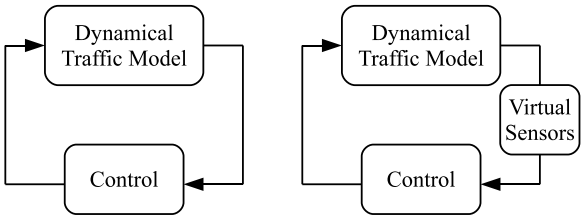

Figure 6. Feedback control system: (a) state feedback; (b) measurement feedback.

Among the available sensing techniques, we distinguish between *point sensors* such as loop detectors and wireless sensors, *mobile sensors* such as GPS equipped vehicles and automatic vehicle location techniques, and *space sensors* such as aerial photography and satellite data.

1. Point sensors are fixed in location along a roadway and measure vehicles passing through this location throughout the time for which they are active.

2. Mobile sensors in vehicles move with the traffic flow in space-time and collect the time stamped position (and speed) of the vehicles.

3. Space sensors can take snapshots of traffic at a given instant of time and repeat such snapshots at multiple time instants.

We model point sensors and mobile sensors. Point sensor is assigned to a link and its position within this link is defined. A link may have multiple point sensors assigned to it. Specific sensor model may implement either loop detector or a Sensys wireless sensor [16]. The measurements provided by a loop detector model are vehicle counts and, possibly, speeds. Data from Sensys sensors can be processed to obtain traffic density in in a link, as described in [12]. A mobile sensor is assigned to a route between given origin and destination. It represents a probe vehicle. These probe vehicles are "phantoms" in the sense that they do not affect the density and flow quantities produced by the original traffic model. A mobile sensor reports its current link together with its position and speed within this link. The intended use of mobile sensors is to compute actual travel time for certain routes as the system evolves in time.

Another purpose of the virtual sensors is to serve as interfaces to the real measurement devices communicating directly to the equipment in the field or to the traffic control center and collecting raw measurement data in real time, while the model (2.1)-(2.7) is used as a dynamical filter for these data before feeding back to the closed-loop traffic controllers. This dynamical filter is described in the next Section.

5. Traffic State Estimation and Prediction

The objectives of dynamic filtering of the measurement data are (1) to provide a better quality feedback for closed-loop controllers; (2) to detect faulty sensors as early as possible; and (3) to help determine initial conditions for the model (2.1)-(2.7) used for the short term prediction in the real time decision support system.

The set-valued estimation of freeway traffic density using Cell Transmission Model was discussed in [7]. This result can be extended to the case of road network. We assume that demands $r_l(t)$ at source links are known with some uncertainty, more precisely, they are constrained by a box $r_l^-(t) \le r_l(t) \le r_l^+(t)$ ($r_l^-(t)$ and $r_l^+(t)$ are known). The other assumption is that the link capacities F_l lie within given intervals $F_l^- \le F_l \le F_l^+$ (F_l^- and F_l^+ are known). Accordingly, denote

$$\overline{\rho}_l^+ = \frac{F_l^+}{w_l} + \frac{F_l^+}{v_l} \quad \text{and} \quad \overline{\rho}_l^- = \frac{F_l^-}{w_l} + \frac{F_l^-}{v_l}. \tag{5.1}$$

Noisy measurements of the output flow

$$y_l^{(f)}(t) = f^d{}_l(t) + \omega_l^{(f)} f(t), \tag{5.2}$$

and speed

$$y_l^{(V)}(t) = V_l(t) + \omega_l^{(V)}(t), \tag{5.3}$$

are available at each link. Here $\omega_l^{(f)}(t) \in [-\omega_l^{0,(f)}(t), \omega_l^{0,(f)}(t)]$ is the flow measurement noise, $\omega_l^{(V)}(t) \in [-\omega_l^{0,(V)}(t), \omega_l^{0,(V)}(t)]$ is the speed measurement noise, and bounds $\omega_l^{0,(f)}(t)$ and $\omega_l^{0,(V)}(t)$ are known. Thus, for each link we get an estimate of the density coming from the measurements:

$$\hat{\rho}_l^-(t) \le \hat{\rho}_l(t) \le \hat{\rho}_l^+(t), \tag{5.4}$$

where

$$\hat{\rho}_l^-(t) = \frac{y_l^{(f)}(t) - \omega_l^{0,(f)}(t)}{y_l^V(t) + \omega_l^{0,(V)}(t)}, \quad \hat{\rho}_l^+(t) = \frac{y_l^{(f)}(t) + \omega_l^{0,(f)}(t)}{y_l^{(V)}(t) - \omega_l^{0,(V)}(t)}. \tag{5.5}$$

Define state bounds update equations for each link l:

$$\rho_l^-(t + \Delta t) = \rho_l^-(t) + \frac{\Delta t}{\Delta x_l} \left(f^u{}_l^-(t) - f^d{}_l^+(t) \right), \tag{5.6}$$

and

$$\rho_l^+(t + \Delta t) = \rho_l^+(t) + \frac{\Delta t}{\Delta x_l} \left(f^u{}_l^+(t) - f^d{}_l^-(t) \right). \tag{5.7}$$

For sources, $f^u{}_l^-(t) = r_l^-(t)$ and $f^u{}_l^+(t) = r_l^+(t)$.
For sinks, $f^d{}_l^-(t) = v_l \rho_l^-(t) \min\left\{1, \frac{F_l^-}{v_l \rho_l^-(t)}\right\}$ and $f^d{}_l^+(t) = v_l \rho_l^+(t) \min\left\{1, \frac{F_l^+}{v_l \rho_l^+(t)}\right\}$.
Otherwise, $f^u{}_l^-(t)$ and $f^u{}_l^+(t)$ are determined by the begin node, and $f^d{}_l^-(t)$ and $f^d{}_l^+(t)$ are determined by the end node. Lower input/output flow bounds $f^d{}_l^-(t)$ and $f^u{}_l^-(t)$ are computed using steps 1-7 from Section 2.a with slight modifications. For a node with input links $i = 1..m$ and output links $j = 1..n$, these modified steps are as follows.

1. Compute lower supply bound for each output:
$$s_j^-(t) = \min\left\{F_j^-, w_j\left(\overline{\rho}_j^- - \rho_j^+(t)\right)\right\}, \quad j = 1..n. \tag{5.8}$$
2. Set index $q = 0$.
3. Compute lower input demand bounds:
$$\tilde{d}_i^{-[q]}(t) = v_i \rho_i^-(t) \min\left\{1, \frac{F_i^-}{v_i \rho_i^-(t)}, \frac{C_i(t, \boldsymbol{\rho}^-(t))}{v_i \rho_i^-(t)}\right\}, \quad i = 1..m. \tag{5.9}$$
4. Compute lower output demand bounds:
$$d_j^{-[q]}(t) = \sum_{i=1}^{m} \beta_{ij}(t) \tilde{d}_i^{-[q]}(t), \quad j = 1..n. \tag{5.10}$$
5. For $q = 1..n$, repeat
   (a) scale down lower input demand bounds according to the lower output supply bounds if necessary:
$$\tilde{d}_i^{-[q]}(t) = \begin{cases} \tilde{d}_i^{-[q-1]}(t), \text{ if } \beta_{iq}(t) = 0 \\ \tilde{d}_i^{-[q-1]}(t) \min\left\{1, \frac{s_j^-(t)}{d_j^{-[q-1]}(t)}\right\}, \text{ otherwise} \end{cases}, \; i = 1..m; \tag{5.11}$$
   (b) recompute lower output demand bounds $d_j^{-[q]}(t)$, $j = 1..n$, according to (5.10).
6. Lower bound for a flow leaving the input link i is
$$f^{d}{}_i^-(t) = \tilde{d}_i^{-[n]}(t) \quad i = 1..m. \tag{5.12}$$
7. Lower bound for a flow entering the output link j is
$$f^{u}{}_j^-(t) = \sum_{i=1}^{m} \beta_{ij} \tilde{d}_i^{-[n]}(t), \quad j = 1..n. \tag{5.13}$$

Upper input/output flow bounds $f^{d}{}_l^+(t)$ and $f^{u}{}_l^+(t)$ are obtained through the same procedure by replacing "$-$" superscripts with "$+$" and vice versa.

By definition of $\rho_l(t)$ in (2.1), $\rho_l^-(t)$ in (5.6) and $\rho_l^+(t)$ in (5.7), if $\rho_l^-(0) \le \rho_l(0) \le \rho_l^+(0)$, then $\rho_l^-(t) \le \rho_l(t) \le \rho_l^+(t)$ for $t \ge 0$. Note that $\rho_l^-(t)$ and $\rho_l^+(t)$ must be restricted so that $0 \le \rho_l^-(t)$ and $\rho_l^+(t) \le \overline{\rho}_l^+$. These restrictions are not satisfied automatically in (5.6), (5.7) and must be imposed explicitly every time step. Boundary trajectories $\rho_l^-(\cdot)$ and $\rho_l^+(\cdot)$ are used to filter the incoming measurement data.

Systems (5.6) and (5.7) start evolving at time $t = 0$ with initial conditions $\rho_l^-(0) \le \rho_l^+(0)$ for every link l, possibly the result of previous estimates. If no initial conditions are available, take the flow and speed measurements $y_l^{(f)}(0)$ and $y_l^{(V)}(0)$ for each link, determine $\hat{\rho}_l^-(0)$ and $\hat{\rho}_l^+(0)$ from (5.5). Systems (5.6) and (5.7) evolve in time until time step $\tau > 0$ when the results of new measurements, $\hat{\rho}_l^-(\tau)$ and $\hat{\rho}_l^+(\tau)$, arrive. Density bounds $\rho_l^-(\tau)$ and $\rho_l^+(\tau)$ are adjusted according to these measurements:
$$\rho_l^-(\tau) \leftarrow \max\left\{1, \frac{\hat{\rho}_l^-(\tau)}{\rho_l^-(\tau)}\right\} \rho_l^-(\tau), \quad \text{and} \quad \rho_l^+(\tau) \leftarrow \min\left\{1, \frac{\hat{\rho}_l^+(\tau)}{\rho_l^+(\tau)}\right\} \rho_l^+(\tau). \tag{5.14}$$
These corrections make sense only if
$$\left[\rho_l^-(\tau), \rho_l^+(\tau)\right] \bigcap \left[\hat{\rho}_l^-(\tau), \hat{\rho}_l^+(\tau)\right] \neq \emptyset. \tag{5.15}$$

Condition (5.15) must be true in theory. Otherwise, it would mean that we made wrong assumptions about the range of measurement noise. In reality, however, empty intersections do occur. What to do in case condition (5.15) is not satisfied depends on the specific situation. If we trust our model more than the measurements, we should skip the correction (5.14). Moreover, we can use our dynamical filter to detect faulty measurement sensors. If, on the other hand, we believe that the measurement data are reliable, correction (5.14) should be modified:

$$\rho_l^-(\tau) \leftarrow \frac{\hat{\rho}_l^-(\tau)}{\rho_l^-(\tau)}\rho_l^-(\tau), \quad \text{and} \quad \rho_l^+(\tau) \leftarrow \frac{\hat{\rho}_l^+(\tau)}{\rho_l^+(\tau)}\rho_l^+(\tau). \tag{5.16}$$

Once the lower bound $\rho_l^-(\tau)$ is corrected according to (5.14) or (5.16), we must check that for each link $\rho_l^-(\tau) \leq \overline{\rho}_l^-$. If for some link this inequality does not hold, there are two alternative ways to proceed. The first is to modify $\rho_l^-(\tau)$:

$$\rho_l^-(\tau) \leftarrow \frac{\overline{\rho}_l^-}{\rho_l^-(\tau)}\rho_l^-(\tau). \tag{5.17}$$

The alternative is to modify the lower capacity bound of the link:

$$F_l^- \leftarrow \frac{\rho_l^-(\tau)}{\overline{\rho}_l^-}F_l^-, \tag{5.18}$$

and then adjust jam density $\overline{\rho}^-$ according to (5.1). Once the corrections (5.14)-(5.17) are applied, the density bounds $\rho_l^-(\tau)$ and $\rho_l^+(\tau)$ in every link can be treated as new initial conditions, and starting at these initial conditions, systems (5.6) and (5.7) should run until the next set of measurements arrives, and so on.

Traffic state prediction involves computing only the bounding trajectories $\rho_l^-(\cdot)$ from (5.6) and $\rho_l^+(\cdot)$ from (5.7) without corrections (5.14). Since the difference $\rho_l^+(t) - \rho_l^-(t)$ gets larger as t increases, it makes sense to limit the prediction to one or two hours into the future, continuously recomputing it as time goes by and new measurements arrive.

Prediction results for 25 July 2009, for 25 miles of I-210 West freeway in Southern California from Baseline Road (postmile 52) to junction with I-710 (postmile 27), are shown in Figure 7. Here, 6.00 AM is the current moment. Data before 6 AM comes from measurements and state estimation. At 6 AM traffic behavior is predicted for the next two hours, until 8 AM: lower and upper density bounds are computed for all the freeway links.

Figure 7a is a snapshot of the projected density bounds (lower bound in green, upper bound in red) along the freeway at 7.30 AM (1.5 hours into the future) computed with no traffic flow control at nodes. At the location marked by the ellipse (between postmiles 40 and 35) the projected density uncertainty interval is large, with its upper bound exceeding critical density and lower bound staying in the free flow state, indicating that the system may develop congestion if left to its own devices, or stay in free flow if managed properly. Such locations are primary candidates for aggressive ramp metering (RM).

Figure 7a shows a snapshot of projected density bounds at the same time if ALINEA ramp metering were applied within the marked freeway segment. The size of the projected density interval is significantly reduced: *the controlled system is more predictable than the uncontrolled one*. Figures 7c and 7d show the evolution of the total network delay (including on-ramp queue delay) for the uncontrolled and ALINEA-controlled cases respectively. From 4 to 6 AM the delay is computed from the measurements (blue), and from 6 to 8 AM the predicted delay bounds (lower bound in green, upper bound in red). One can see that ALINEA ramp metering potentially yields a noticeable delay reduction.

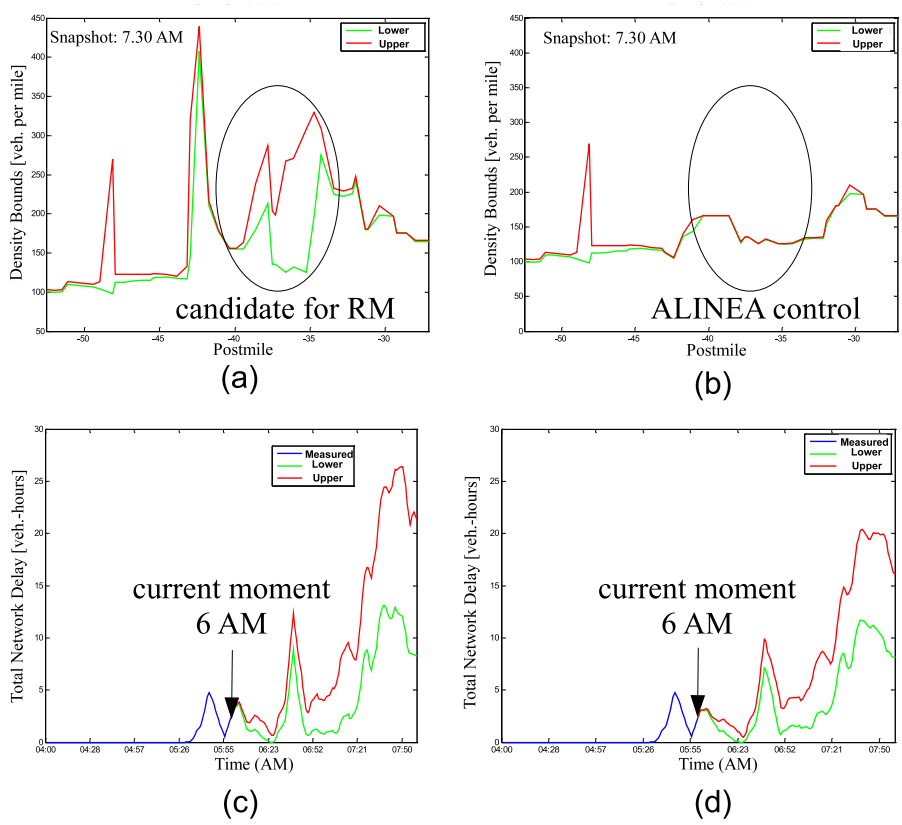

Figure 7. Short term prediction from 6 to 8 AM for I-210 West: (a) projected density bounds for 7.30 AM without ramp metering; (b) projected density bounds for 7.30 AM with ALINEA ramp control; (c) projected bounds for total network delay without ramp metering; (d) projected bounds for total network delay with ALINEA ramp control.

This is just one example. In reality, the traffic operator should test several potential control strategies and apply the most effective one. A macroscopic traffic simulator such as Aurora RNM [1] is able to run a hundred of simulations with preprogrammed scenarios in a matter of several minutes.

6. Conclusion

Adequate historical and real time traffic data that support a fast and trusted simulation engine form the basis for constructing the analytical capability the ATM needs. High simulation speed allows the operator to analyze tens of potential control strategies in a matter of minutes. Therefore, microsimulation is not up to the task. We advocate macroscopic simulation, which while being fast can also be trusted as (1) it adequately captures the dynamics of traffic flow; and (2) all simulation model parameters can be reliably estimated from traffic data. Calibration of the proposed macroscopic model parameters is straightforward when the corresponding data are available. The frequent lack of ramp flow measurements can be partially compensated by imputation of on-ramp demands and off-ramp split ratios.

The system performance under various scenarios and control strategies is evaluated using such measures as traffic speed, actual travel time, which can be computed per link or per route, and VMT, VHT, delay and productivity loss, which can be also be computed for the whole network. For signalized arterial intersections additional

performance measures, such as delay per cycle, queue size, phase utilization, cycle failure, flow to capacity ratio, and progression quality, apply.

Traffic control in our model is actuated at nodes. Local controllers operating on individual input links, node controllers operating on all input links in individual nodes, and complex controllers operating on multiple local, node or other complex controllers, form the controller hierarchy. To simulate a realistic model of a closed-loop traffic control system, we replace the state feedback with the measurement feedback by introducing the concept of virtual sensors. A virtual sensor models a measurement device whose quality may be anywhere between excellent and unsatisfactory. Significantly, it can serve as an interface with field measurement devices during real time operation.

The simulator has three modes of operation. In the operations planning mode scenarios are tested, and control strategies are assessed in terms of their cost and benefits, so that reliable decisions may be made about which strategies to implement. The second mode is the dynamical filter, used in real time to improve the quality of the feedback for the traffic controllers. The third mode is short term prediction, which estimates the uncertainty in the future traffic state based on current measured conditions and the projected demands for the near future (one-two hours) under a variety of implemented control strategies for the purpose of selecting the most suitable one for the predicted situation. An example of I-210 West freeway in Los Angeles illustrates some ATM features based on the presented framework.

The dynamical traffic model, some elements of model building process (eg. GIS data importing), the control framework together with selected local node and complex controllers, and estimation/prediction algorithms are implemented in Aurora RNM [1] and available for download.

7. Acknowledgement

This research was supported by National Science Foundation Award CMMI-0941326 and the California Department of Transportation. We are grateful to members of the TOPL research project [18], especially G. Dervisoglu, G. Gomes, R. Horowitz, A. Muralidharan and R. Sanchez.

References

[1] Aurora RNM Homepage. http://code.google.com/p/aurorarnm.

[2] C. Chen, J. Kwon, A. Skabardonis, and P. Varaiya. Detecting errors and imputing missing data for single loop surveillance systems. *Transportation Research Record*, (1855):160–167, 2003.

[3] C. F. Daganzo. The cell transmission model: A dynamic representation of highway traffic consistent with the hydrodynamic theory. *Transportation Research, B*, 28(4):269–287, 1994.

[4] C. F. Daganzo. The cell transmission model II: Network traffic. *Transportation Research, B*, 29(2):79–93, 1995.

[5] G. Dervisoglu, G. Gomes, J. Kwon, A. Muralidharan, and P. Varaiya. Automatic calibration of the fundamental diagram and empirical observations on capacity. *88 Annual Meeting of the Transportation Research Board, Washington, D.C., USA*, 2008.

[6] C. Diakaki, M. Papageorgiou, and T. McLean. Integrated traffic-responsive urban corridor control strategy in glasgo, scotland. *Transportation Research Record*, (1727):101–111, 2000.

[7] A. A. Kurzhanskiy. Set-valued estimation of freeway traffic density. *Proceedings of the 12th IFAC Symposium on Control in Transportation Systems*, 2009.

[8] A. Muralidharan and R. Horowitz. Imputation of ramp data flow for freeway traffic simulation. *Transportation Research Record*, 2009.

[9] Navteq Corporation. http://www.navteq.com.

[10] OpenStreetMap Project. http://www.openstreetmap.org.

[11] M. Papageorgiou, H. Hadj-Salem, and H. M. Blosseville. ALINEA: A local feedback control law for onramp metering. *Transportation Research Record*, (1320), 1991.

[12] M. Papageorgiou and P. Varaiya. Link vehicle-count — the missing measurement for traffic control. *Proceedings of the 12th IFAC Symposium on Control in Transportation Systems*, 2009.

[13] I. Papamichail, M. Papageorgiou, V. Vong, and J. Gaffney. HERO coordinated ramp metering implemented at monash freeway, australia. *89th Annual Meeting of the Transportation Research Board, Washington, D.C., USA*, 2010.

[14] PeMS Homepage. http://pems.eecs.berkeley.edu.

[15] PORTAL Homepage. http://portal.its.pdx.edu.

[16] Sensys Networks. http://www.sensysnetworks.com.

[17] Tele Atlas. http://www.teleatlas.com.

[18] TOPL Project. http://path.berkeley.edu/topl.